JOURNAL OF GEOPHYSICAL RESEARCH, VOL. 115, B01303, doi:10.1029/2009JB006453, 2010

Seismicity and state of stress in Guerrero segment of the Mexican subduction zone

Javier F. Pacheco[1,2] and Shri K. Singh[1]

Received 10 March 2009; revised 6 October 2009; accepted 20 October 2009; published 27 January 2010.

[1] We take advantage of a relatively dense network of seismic stations in the Guerrero segment of the Mexican subduction zone to study seismicity and state of stress in the region. We combine our results with recent observations on the geometry of the subducted Cocos plate imaged from receiver function (RF) analysis, an ultraslow velocity layer mapped in the upper crust of the subducted slab, and episodic slow slip events (SSEs) and nonvolcanic tremors (NVTs) reported in the region to obtain a comprehensive view of the subduction process. Seismicity and focal mechanisms confirm subduction of the Cocos plate below Mexico at a shallow angle, reaching a depth of 25 km at a distance of 65 km from the trench. The plate begins to unbend at this distance and becomes horizontal at a distance of ~120 km at a depth of 40 km. Some of the highlights of the inslab seismicity are as follows: (1) A cluster of earthquakes in the depth range of 25–45 km, immediately downdip from the strongly coupled part of the plate interface, revealing both downdip compressional and extensional events. This seismicity extends from ~80 to 105 km from the trench and may be attributed to the unbending of the slab. (2) The slab devoid of seismicity in the distance range of ~105–160 km. (3) Sparse inslab seismicity revealing downdip extension in the distance range of 160–240 km. The NVTs are also confined to this distance range. The episodic SSEs occur on the horizontal segment, in the distance range of ~105–240 km, where an ultraslow velocity layer in the upper crust of the slab has been mapped from waveform modeling of converted SP phases. Thus, in the distance range of ~105–160 km, SSEs occur but NVTs and inslab earthquakes are absent. This suggests that metamorphic dehydration reactions in the subducting oceanic crust and upper mantle begin at a distance of ~160 km, giving rise to both the inslab earthquakes and NVTs. No inslab earthquake occurs beyond 240 km. The receiver function images and *P* wave tomography suggest that the slab begins a steep plunge at a distance of ~310 km, reaching a depth of 500 km around 340 km from the trench. The negative buoyancy of such a slab should give rise to large extensional stress in the slab. Yet inslab seismicity is remarkably low, which may be explained by a slab that is not continuous up to a depth of 500 km, but is broken at a shallower depth. The resulting slab window may permit subslab material to flow through the gap. This may provide an explanation for the recent rift-related basalts found near Mexico City. The fore-arc, upper plate seismicity, which during the period of study (1995–2007) consisted of a moderate earthquake (M_w 5.8) near the coast (H = 12 km), its numerous aftershocks, and two shallow events farther inland, demonstrates a trench-normal extension in the upper plate near this convergent margin, a state of stress that may be explained by tectonic erosion and/or seaward retreat of the trench. Seismicity, location of the mantle wedge, and rupture areas of Mexican earthquakes suggest that the downdip limit of rupture during large/great earthquakes in Guerrero may be 105 ± 15 km. Shallow-dipping, interplate thrust earthquakes are not the only type of events that affect the seismic hazard in the region. The magnitudes of inslab downdip compressional and extensional earthquakes that occur within ~20 km inland from the coast, in the depth range of 25–45 km, may reach 6.5 and

[1]Instituto de Geofísica, Universidad Nacional Autónoma de México, Ciudad Universitaria, México D. F., México.
[2]Now at Observatorio Vulcanológico y Sismológico de Costa Rica, Universidad Nacional Autónoma, Costa Rica.

0148-0227/10/2009JB006453$09.00

7.5, respectively. In addition, we now identify normal-faulting earthquakes in the upper plate. These sources need to be taken into account in the hazard estimation.

Citation: Pacheco, J. F., and S. K. Singh (2010), Seismicity and state of stress in Guerrero segment of the Mexican subduction zone, *J. Geophys. Res.*, *115*, B01303, doi:10.1029/2009JB006453.

1. Introduction

[2] An accurate knowledge of seismicity and state of stress in subduction zones is critical in developing models of slab subduction and realistic estimation of seismic hazard. This, however, requires a dense local seismic network. The only region along the Mexican subduction zone where such a study is possible is the Guerrero segment (Figure 1). The recognition that the region is a mature seismic gap [*Kelleher et al.*, 1973; *Singh et al.*, 1981] led to the installation of the Guerrero Accelerographic Array in 1985 [*Anderson et al.*, 1994]. The Michoacan earthquake of 1985 (M_w 8.0), which ruptured the plate interface NW of the seismic gap and caused unprecedented damage to Mexico City, gave rise to heightened concern of a similar earthquake in the Guerrero seismic gap. As a result, the accelerographic network in the region was strengthened. A seismic network was also operated during 1987–1993 to monitor the seismicity and to map the geometry of the subducted Cocos plate beneath the region.

[3] A seismicity study, based on the data from the local network, revealed that the oceanic Cocos plate dips at shallow angle to a depth of about 40 km [*Suárez et al.*, 1990]. Because of the lack of microseismicity inland, the geometry of the subducted slab could not be traced beyond 20 km from the coast (80 km from the trench). The slab trajectory farther inland was inferred from hypocenter and focal mechanism of earthquakes of 6 June 1964 and 2 July 1968 below central Mexico, which had been studied previously using teleseismic data by *González-Ruiz* [1986] and *Molnar and Sykes* [1969], respectively. The composite data suggested that the slab becomes subhorizontal beyond ~80 km from the trench, reaching a depth of 50 km about 200 km inland [*Suárez et al.*, 1990]. Since the inslab seismicity ceases completely farther inland, it was speculated that beyond 200 km, the slab plunges steeply, reaching a depth of 100 km below the active volcano of Popocatepetl. *Singh and Pardo* [1993] determined depths and focal mechanisms of small earthquakes in central Mexico from local seismic and accelerographic stations. These data, along with some previous ones, supported the geometry of the plate inferred by *Suárez et al.* [1990]. The seismicity in the overriding continental plate is low; a few events in the fore arc analyzed by *Singh and Pardo* [1993] suggested that it is in extension. They suggested that the extensional stress regime of upper plate could be a consequence of seaward retreat of the trench or tectonic erosion of the leading edge of the continent. *Pardo and Suárez* [1995] studied the geometry of the subducted Cocos plate below Mexico using accurately determined hypocenters based on local or teleseismic data (see inset in Figure 1). The seismicity and focal mechanisms reconfirmed the subhorizontal trajectory of the slab below Guerrero.

[4] While the studies mentioned above establish the basic geometry of the Wadati-Benioff zone below Guerrero, some details remain unresolved:

[5] 1. *Suárez et al.* [1990] identify two bands of seismicity near the coast. The seismicity of the coastal band is ~35 km wide and occurs in the depth range of 10–25 km. The second band is located farther inland, in the depth range of 32–42 km. Composite focal mechanisms reveal shallow thrust faulting and normal faulting for the events in the coastal and inland bands, respectively. The stress axes of the normal-faulting events suggest downdip tension. In the last 15 years, there have been several moderate/large inslab earthquakes in Mexico which were located near the coast, below or close to the downdip edge of the coupled plate interface. The focal mechanisms of some of these events exhibit downdip extension (e.g., Michoacan earthquake of 11 January 1997, M_w 7.1 [*Santoyo et al.*, 2005]; Oaxaca earthquake of 30 September 1999, M_w 7.4 [*Singh et al.*, 2000b]), while others indicate downdip compression (e.g., Atoyac earthquake of 13 April 2007, M_w 5.9 [*Singh et al.*, 2007]). Is the occurrence of these earthquakes in agreement with the state of stress in Guerrero deduced from small earthquakes? Do both types of earthquakes occur in the slab just below or immediately downdip from the coupled interface?

[6] 2. If hypocenters of 100 km wide regions in Guerrero are projected on vertical planes along the direction of convergence, they exhibit continuous, albeit, low seismicity in the slab in the distance range of 80–200 km from the trench. If accurately located hypocenters of a less wide region (~50 km) are considered, would they still show continuous seismicity? In other words, is there a subhorizontal segment of the slab that is devoid of seismicity?

[7] 3. The evidence of extensional stress regime in the overriding plate came from a few events that may not have been well located. Do focal mechanisms of recent, well-located events support this state of stress?

[8] As the seismic hazard from the Guerrero seismic gap still persists, the accelerographic array has been upgraded and new permanent broadband seismic stations have been deployed in the region. In a collaborative project among Universidad Nacional Autónoma de México (UNAM), California Institute of Technology (Caltech), and University of California, Los Angeles (UCLA), a portable array of 100 broadband seismographs, spaced 5 km apart, was operated between Acapulco and Tampico during 2005–2007. This project is called the Middle America Seismic Experiment (MASE) [*Clayton et al.*, 2007]. In the present study, we use the data from all of these networks to locate small to moderate earthquakes that occurred in the region during 1995–2007 and determine their focal mechanisms from waveform inversion. The new data better characterize the state of stress in the subducted slab and the upper continental plate. We use this information, along with the image of the Cocos plate recently obtained from the analysis of RFs using the MASE data [*Pérez-Campos et al.*, 2008], the evidence showing presence of a thin (~3–5 km) ultraslow velocity, high pore fluid pressure (HPFP) layer at the top of

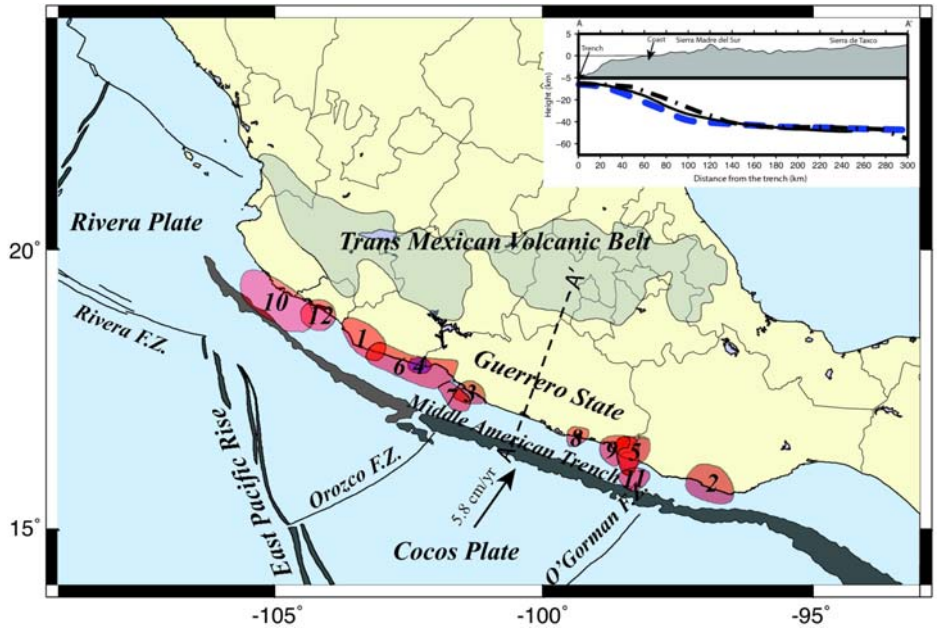

Figure 1. Main tectonic features of the Guerrero segment of the Mexican subduction zone. Seismicity and volcanism in the region are related to the subduction of Cocos plate below Mexico at a rate of ~6 cm/yr. Mexico is part of the North American plate. Arrow shows the direction of relative convergence. Rupture areas of recent large to great earthquakes along the Mexican subduction zone are outlined. Sections along AA′ of the plate interface inferred in this study (thick dashed blue line), from *Suárez et al.* [1990] (continuous line), and from *Singh and Pardo* [1993] (dash-dotted line) are shown in the inset, where the trench and the coast are marked. The coast is located 60 km from the trench. In the text, the distances are often referred with respect to the trench but sometimes with respect to the coast.

the subducted crust of the slab [*Song et al.*, 2009], the reported episodic slow slip events (SSEs) [*Kostoglodov et al.*, 2003; *Iglesias et al.*, 2004; *Yoshioka et al.*, 2004; *Larson et al.*, 2007; *Correa-Mora et al.*, 2009], and nonvolcanic tremors [*Payero et al.*, 2008], to understand the dynamics of subduction in the region. Additionally, our results identify different types of seismic sources that need to be taken into account in a realistic estimation of seismic hazard in Guerrero, Mexico.

2. New Seismic Data and Data Processing

[9] Between 1993 and 1995, most of the accelerographs in Guerrero (Figure 2) were upgraded to 18- or 19-bit digitizers. This permits recordings of smaller-magnitude earthquakes with higher signal-to-noise ratio. In 1994 and 1995, four permanent broadband seismic stations (PLIG, CAIG, ZIIG, and PNIG) were installed in the region (Figure 2). As shown in Figure 2, the linear MASE array, which was in operation between 2005 and 2007, crosses the region along a profile parallel to the direction of plate convergence. Short-period stations, and other nondigital accelerographs and temporary stations used for *P* wave arrival time readings and locations are not shown in Figure 2.

[10] We searched for velocity and acceleration records of all earthquakes located by the National Mexican Seismological Service (SSN) (http://www.ssn.unam.mx) in the Guerrero region between 1995 and 2007, and added them to the SSN database. Events were relocated by converting the seismograms to the SeiSan format [*Havskov and Ottemöller*, 1999] and, within the program, applying the Hypocenter algorithm of *Lienert and Havskov* [1995] with a crustal structure modified from *Iglesias et al.* [2001]. We use clear *P* wave arrival time readings from all stations and clear *S* wave arrival time readings only for stations located within 80 km distance from the epicenter. The 1-D crustal

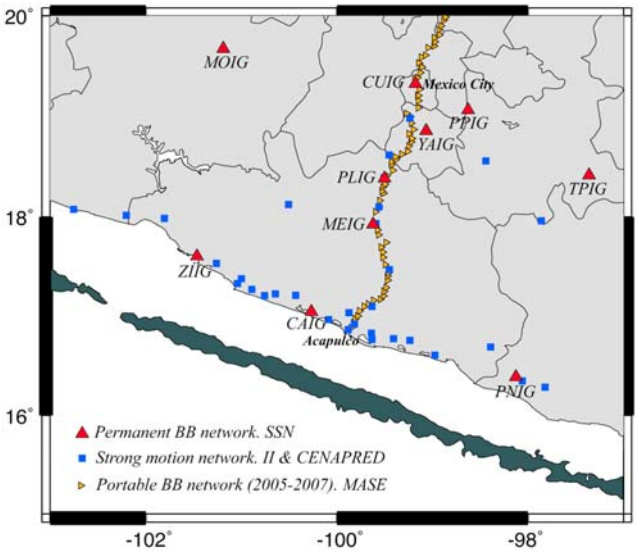

Figure 2. Seismic stations in the Guerrero region. Large red triangles indicate permanent broadband stations; blue squares indicate accelerographic stations; small yellow triangles indicate broadband portable array deployed during the Middle America Subduction Experiment (MASE).

model for Guerrero gives large travel time errors for *S* waves at larger distances. Events were rejected if the hypocenter solutions had a root-mean-square (RMS) residual >1 s. We choose events located within the state of Guerrero and recorded by at least one digital station situated within a distance smaller than the earthquake depth. The last restriction was relaxed for moderate to large events listed in the global centroid moment tensor (CMT) catalog (http://www.globalcmt.org) and located at the edges of the Guerrero state. These events have larger depth errors, but they are not used in the cross section. Given the station distribution (Figure 2), many events did not produce a nearby recording and, hence, were rejected. These filters left a total of 275 events between 15°N and 19°N and 98°W and 102°W for further analysis.

[11] Regional centroid moment tensor solutions were determined for moderate events recorded at broadband stations of the SSN with high signal-to-noise ratio at long periods (10–100 s), using the algorithm of *Randall et al.* [1995], and processed according to *Pacheco and Singh* [1998]. Centroid depth for these events was estimated by finding the smallest least squares residual from the inversion of the moment tensor computed at discrete depths. Depth sensitivity is low, as surface waves are the dominant feature of the regional seismograms. The solutions were constrained to a double-couple source. Focal mechanism and seismic moment of well-located small events, recorded at short distances, were determined by inverting near-source displacement seismograms following the procedure described by *Singh et al.* [2000a] and *Pacheco et al.* [1999], with constrains imposed by first-motion data. Here, depths were fixed to the hypocentral depths obtained from the location algorithm.

[12] Some small events had to be dropped because they had too small signal-to-noise ratio to yield a reliable focal mechanism. Our analysis is based on 132 earthquakes (Table 1) that remained after applying the criteria mentioned above. These earthquakes have hypocenter RMS residuals <0.5 s in the central part of Guerrero and <0.8 s at the edges. The location error varies over time and space. The formal horizontal and vertical location errors of earthquakes in Table 1, without data from the MASE array, are ~5 km for events along the coast and within the area of about 50 km wide at both sides of the strong motion attenuation line that goes from Acapulco to Mexico City. The MASE array lies along this attenuation line. These errors diminish considerably during MASE's operation. The errors are larger away from the attenuation line. Regional CMT solutions for these events have a weighted least squares error smaller than 0.5, and compensated linear vector dipole (CLVD) component of less than 70%.

[13] Henceforth, in this paper, we shall use epicenters and depths of the 132 earthquakes obtained from the location algorithm. Table 1 lists fault plane solutions determined in this study and those reported in the Global CMT catalog [*Dziewonski and Woodhouse*, 1983]. For completeness, the table gives the corresponding centroid depths. Global CMT solution is available for 40 out of the 132 earthquakes listed in the table and regional CMT solution is available for 38 out of these 40 events. We note that the Global and regional CMT solutions are very similar. The regional CMT inversion uses a point source approximation which starts to fail for events with $M_w > 5.7$. This is reflected in magnitude saturation and phase shifts that result in a large CLVD component. For these events, and those that occurred before 1998 when the Mexican broadband network was sparse, we prefer the Global CMT solution if available. For southern central Mexico, the Global CMT catalog is complete for $M_w \geq 5.3$. Presumably, the recordings of smaller-magnitude earthquakes have poor signal-to-noise ratio at teleseismic distances. For this reason, we prefer the regional CMT solution for events since 1998 with $M_w < 5.3$, unless the Global CMT better fits the first-motion data. In Table 1, the preferred solution of these events is listed first. However, for events since 1998, with $5.3 \leq M_w \leq 5.7$, we have no preference between the Global and regional CMT solutions and the first solution listed in the table is random. In any case, the solutions are sufficiently similar so that the conclusions reached in this paper are independent of the choice.

3. Results

[14] To facilitate the classification of the earthquakes listed in Table 1 in different groups, we plotted epicenters of the events along with their focal mechanisms, and projected the hypocenters on vertical planes oriented in the direction perpendicular to the trench. Figure 3 illustrates interplate and inslab earthquakes while the earthquakes in the overriding plate are plotted in Figure 4. The network coverage (Figure 2) permits reliable location of the earthquakes in the area covered by the two rectangles in Figure 5a. Figures 5b and 5c show the projection of the hypocenters and focal mechanisms of the events enclosed in the boxes on planes AA′ and BB′. Note that event 63, which is located outside the box, has also been projected on section AA′. This is the farthest event from the coast on this section. Although in further analysis and discussion, we will take this event as if it were located in the box, the true location of the event should be kept in mind.

3.1. Interplate and Inslab Earthquakes

[15] Four types of focal mechanism can be identified for this group of earthquakes (Figures 3 and 5): (1) shallow, low-angle thrust earthquakes (Figure 3a), (2) earthquakes that exhibit downdip tension (Figure 3b), (3) events that reveal downdip compression (Figure 3c), and (4) events with unusual strike-slip or normal fault mechanism with strike oriented at an oblique angle to the trench.

[16] Shallow thrust events (Figure 3a) occur between the trench and the coast on the plate interface. Most of the shallow events studied here are located close to the coast as we mostly analyzed earthquakes with at least one near-source recording. The events offshore are mostly moderate earthquakes reported in the Global CMT catalog. The depth sections (Figure 5) suggest that the slab enters below the continent with a dip of about 15°. The depth of the shallow thrust events reaches ~25 km near the coast (Table 1 and Figure 5). This type of event ceases to occur beyond ~65 km from the trench (~5 km inland from the coast).

[17] Immediately below the plate interface, where the shallow thrust events end, a cluster of seismicity in the depth range of 25–45 km occurs. These events reveal both downdip compression and downdip extension. On sections

Table 1. List of Earthquakes Analyzed in This Study and Their Source Parameters

Event	Date[a]	Time (UT)	Seconds	Longitude	Latitude	Depth (km)	Mechanism Strike/Dip/Rake	M_w	Centroid Depth (km)	Source[b]
1	19950427	0642	21.11	−101.846	17.895	52.6	293/73/71	5.2	41.6	2
							285/86/75	5.2	45.0	1
2	19960101	1715	16.43	−99.544	17.055	38.3	123/59/−71	3.7	38.3	1
3	19960313	2104	19.60	−99.118	16.616	25.0	297/62/85	5.1	29.4	2
							298/65/78	4.8	25.0	1
4	19960423	0653	34.03	−101.586	17.081	21.9	228/65/35	5.5	36.8	2
							222/53/11	5.4	15.0	1
5	19960429	1835	19.90	−100.706	17.323	38.5	301/78/107	4.0	38.0	1
6	19960508	0124	43.11	−100.184	16.835	13.5	257/29/45	4.1	13.0	1
7	19960715	2123	34.50	−101.241	17.293	18.7	297/21/93	6.6	22.4	2
							269/90/−87	6.4	25.0	1
8	19960718	0816	43.35	−101.254	17.379	20.0	285/19/81	5.4	26.2	2
							290/19/91/	5.1	20.0	1
9	19960719	0900	53.51	−100.371	17.276	44.9	320/34/−59	4.7	35.0	1
10	19960827	1255	33.77	−99.320	16.659	21.8	250/42/55	4.2	22.0	1
11	19970121	2119	59.19	−98.210	16.404	19.9	296/10/80	5.3	21.0	3
							320/17/89	5.2	15.0	1
							281/26/49	5.5	39.7	2
12	19970322	0349	14.76	−99.778	16.993	37.8	116/83/−119	4.7	37.0	1
13	19970403	2122	30.81	−98.328	17.995	33.4	258/27/−87	5.2	51.7	2
							267/29/−80	5.1	50.0	1
14	19970508	1558	28.31	−100.433	17.305	37.6	315/28/−69	5.0	35.0	1
15	19970519	1123	52.11	−100.451	17.271	39.4	113/88/−88	4.3	30.0	1
16	19970522	0750	54.14	−101.869	18.371	78.6	269/62/−96	6.5	55.5	2
							265/65/−93	6.2	55.0	1
17	19970628	2329	55.94	−99.692	17.034	29.7	284/50/80	3.3	29.7	1
18	19970711	2223	33.50	−99.630	16.783	17.1	277/32/77	4.2	15.0	1
19	19970719	0734	37.30	−100.460	17.282	38.9	318/19/−62	4.7	35.0	1
20	19971216	1148	29.00	−99.106	16.021	5.0	260/18/64	5.9	16.0	2
							283/38/87	5.5	5.0	1
21	19971222	0522	8.10	−101.152	17.231	16.3	292/29/89	5.4	15.0	1
23	19980225	1709	33.10	−101.095	17.272	18.1	294/28/92	4.8	20.0	1
24	19980301	1358	34.91	−99.450	17.002	25.0	312/71/113	3.6	25.0	1
25	19980305	1451	3.50	−100.221	16.850	16.0	280/65/90	3.9	16.0	1
26	19980311	1413	11.00	−100.066	17.114	36.1	46/55/−15	3.7	36.0	1
27	19980420	2259	15.50	−101.272	18.338	86.1	290/61/−86	5.9	59.6	2
28	19980509	1703	12.70	−101.270	17.444	16.7	296/36/95	5.2	36.2	2
							289/32/85	5.1	15.0	1
29	19980516	1741	53.95	−101.381	17.210	11.1	313/22/102	5.2	33.0	2
							287/30/86	4.8	25.0	1
30	19980524	0930	31.20	−99.893	17.012	5.6	96/69/−76	2.9	6.0	1
31	19980601	0759	32.33	−100.095	16.831	17.3	279/33/78	4.6	20.0	1
32	19980627	1622	43.74	−100.890	17.389	36.1	40/11/−6	3.5	34.0	1
33	19980705	1955	5.60	−100.145	16.781	12.8	281/30/76	5.3	15.0	1
							261/21/48	5.3	37.6	2
34	19980711	0521	12.70	−101.434	17.322	17.5	275/16/60	5.4	24.1	2
							315/23/116	5.1	20.0	1
35	19980712	0811	26.52	−100.478	16.813	10.0	311/31/91	5.5	10.0	1
							269/22/37	5.5	15.0	2
36	19980717	1118	1.92	−100.096	16.969	27.4	341/85/158	4.9	25.0	1
37	19980805	1649	57.40	−100.225	17.974	56.6	346/48/−42	4.6	55.0	1
38	19980809	1618	5.26	−100.263	16.833	15.2	340/24/154	4.1	16.0	1
39	19980824	1953	39.62	−99.844	17.105	37.1	283/69/75	3.9	37.0	1
40	19980907	0653	17.57	−99.667	16.804	25.0	247/47/59	3.5	25.0	1
41	19980930	2158	38.00	−99.073	16.456	16.6	340/62/120	4.1	13.0	1
42	19981127	1529	30.37	−99.516	16.971	33.3	305/77/130	4.1	37.0	1
44	19990215	0500	42.30	−99.308	16.541	27.3	79/71/−37	4.2	10.0	1
45	19990219	2158	1.80	−100.704	17.300	37.7	264/85/67	3.9	37.0	1
46	19990302	2045	12.50	−99.601	17.068	34.3	295/65/81	4.0	34.0	1
47	19990408	2219	48.77	−100.008	17.031	8.2	270/30/−65	3.5	10.0	1
48	19990425	0308	56.60	−100.781	17.256	35.2	328/26/−51	4.4	30.0	1
49	19990530	0958	42.55	−100.732	17.336	40.9	269/85/91	4.3	36.0	1
50	19990813	0314	50.60	−99.208	16.614	19.6	236/49/35	3.9	16.0	1
51	19990816	0409	45.92	−99.873	17.155	36.5	273/70/137	3.7	36.0	1
52	19990922	0837	12.02	−100.806	17.092	16.5	321/19/81	4.1	16.0	1
53	19991027	0253	54.35	−99.764	17.021	33.5	20/81/−14	3.7	37.0	1
54	19991108	0236	47.47	−100.754	17.370	34.4	283/85/94	4.4	40.0	1
55	19991119	0456	29.28	−99.427	16.741	23.4	313/28/108	3.8	28.0	1
56	19991229	0519	45.30	−101.620	18.044	49.7	260/22/−129	5.9	50.0	2
							270/30/−129	5.7	45.0	1
57	20000126	1924	52.30	−99.502	16.534	13.4	291/29/90	4.8	10.0	1
58	20000308	2241	4.15	−100.091	16.921	27.9	310/49/115	3.6	28.0	1

Table 1. (continued)

Event	Date[a]	Time (UT)	Seconds	Longitude	Latitude	Depth (km)	Mechanism Strike/Dip/Rake	M_w	Centroid Depth (km)	Source[b]
59	20000318	0050	57.70	−99.281	17.182	33.3	298/77/103	5.0	35.0	1
60	20000321	1828	11.20	−99.041	16.570	16.7	269/34/66	4.8	18.0	1
61	20000415	0145	5.10	−100.345	16.941	22.2	292/46/92	4.5	15.0	1
62	20000515	0726	8.90	−100.804	17.105	17.4	312/36/120	4.5	17.0	1
63	20000721	0613	39.12	−98.975	18.116	53.2	289/33/−81	5.8	56.0	2
							295/28/−88	5.9	55.0	1
64	20000928	1719	2.10	−100.688	17.272	36.0	52/61/−12	3.8	35.0	1
65	20001130	0858	55.60	−101.109	17.190	11.8	279/50/70	4.2	20.0	1
66	20010305	1017	35.30	−100.100	17.093	37.0	250/16/−131	5.1	25.0	1
67	20010306	2157	55.60	−100.100	17.100	36.7	340/30/−49	5.0	25.0	1
68	20010904	0326	28.30	−98.378	16.261	16.6	293/20/90	5.0	15.0	1
							286/23/69	5.2	33.7	2
69	20011008	0339	18.35	−100.096	16.984	11.9	263/39/−107	5.8	15.0	2
							265/47/−101	5.8	8.0	1
70	20011008	0715	59.15	−100.164	16.945	14.1	118/45/−45	4.4	5.0	1
71	20011009	0034	21.61	−100.088	17.061	7.8	274/51/−92	4.4	8.0	1
72	20011029	0523	11.40	−100.206	16.987	11.2	102/65/−78	4.9	5.0	1
							240/44/−116	5.0	15.0	1
73	20011105	0322	15.39	−99.747	16.813	19.2	274/27/75	4.1	20.0	1
74	20011110	1709	14.90	−98.295	16.053	9.6	243/10/69	5.4	10.0	2
							261/15/96	5.2	10.0	1
75	20011123	0641	37.12	−100.161	17.045	8.7	258/54/−80	4.6	8.0	1
76	20020102	0128	44.80	−101.766	18.700	66.2	196/14/−11	4.7	60.0	1
77	20020120	0834	35.86	−100.055	17.040	6.5	298/68/−76	4.3	5.0	1
78	20020123	0924	0.23	−100.025	17.066	3.0	102/42/−80	4.1	10.0	1
79	20020123	1149	2.34	−100.025	17.067	6.0	293/58/−72	3.8	10.0	1
80	20020214	0505	21.72	−100.124	17.059	10.4	109/55/−59	4.3	5.0	1
81	20020214	1530	22.24	−100.118	17.077	1.4	268/50/−92	4.5	5.0	1
82	20020217	0410	19.96	−99.953	17.075	31.1	290/87/94	4.4	20.0	1
83	20020219	0607	27.56	−100.035	17.040	10.4	257/61/−97	4.0	10.0	1
84	20020221	1921	50.70	−99.646	17.019	37.4	304/87/131	3.9	38.0	1
85	20020305	1116	47.30	−100.141	16.438	11.7	310/36/109	4.4	10.0	1
86	20020307	2208	10.70	−100.149	17.021	11.1	96/28/−87	4.1	10.0	1
87	20020418	0502	43.10	−101.093	16.688	12.7	291/9/89	6.7	15.0	2
							332/28/123	6.3	10.0	1
88	20020418	1100	41.10	−101.174	17.141	22.3	281/63/80	5.0	10.0	1
							244/31/32	5.1	20.0	1
89	20020418	1757	23.40	−101.414	16.945	23.7	273/17/81	5.9	44.2	2
90	20020428	1750	10.50	−99.646	16.801	17.7	280/32/70	4.4	20.0	1
91	20020503	1247	2.51	−100.129	16.979	9.1	317/49/−19	3.9	10.0	1
92	20020511	0249	34.60	−100.120	17.119	34.9	287/80/80	4.0	34.0	1
93	20020528	2133	55.90	−99.543	16.261	23.4	291/34/87	4.6	5.0	1
94	20020622	1015	33.96	−99.696	17.185	44.5	292/80/133	4.3	45.0	1
95	20020628	1808	32.80	−99.825	16.768	17.3	322/12/106	4.3	17.0	1
96	20020829	0847	44.20	−98.911	16.813	28.8	274/46/90	4.0	25.0	1
97	20020830	2111	41.80	−100.942	16.722	8.0	314/35/140	5.0	8.0	1
							254/30/44	5.2	24.2	2
98	20020925	1814	46.90	−100.133	16.810	17.1	287/30/84	5.1	15.0	1
							271/22/61	5.3	19.0	2
99	20020927	0704	57.00	−100.524	17.266	34.5	290/60/87	5.0	25.0	1
							268/45/72	5.1	36.4	2
100	20021210	0309	33.50	−101.272	17.747	38.7	220/15/−15	5.3	30.0	1
							250/26/1	5.4	66.7	2
101	20030110	0208	1.10	−100.355	17.019	32.3	259/50/56	5.1	20.0	1
							241/49/35	5.2	44.7	2
102	20030131	1556	50.60	−100.129	17.045	12.3	112/56/−34	4.4	5.0	1
103	20030207	0741	16.80	−100.140	17.080	0.9	102/34/−43	3.8	5.0	1
104	20030327	0744	21.60	−101.792	18.005	44.4	121/89/−76	5.2	25.0	1
							310/79/98	5.2	30.9	2
105	20030421	0756	26.10	−101.260	17.503	35.8	210/37/−15	4.5	35.0	1
106	20030516	0909	23.40	−101.241	18.292	61.7	292/67/−79	4.7	55.0	1
							297/56/−61	5.0	84.3	2
107	20030517	0716	2.60	−99.094	16.753	25.0	309/33/117	4.0	20.0	1
108	20030622	0152	36.20	−99.634	16.797	21.3	276/37/81	4.2	18.0	1
109	20030721	2353	43.10	−101.049	18.468	67.7	289/52/−89	5.1	62.4	2
							134/37/−54	4.9	40.0	1
110	20031119	1350	26.70	−99.538	17.861	57.3	306/44/−52	5.1	50.0	1
							277/37/−69	5.2	69.3	2
111	20040101	2331	47.50	−101.500	17.344	25.0	299/13/92	6.0	15.0	2
							302/29/94	5.7	15.0	1
112	20040101	2357	59.90	−101.464	17.340	25.0	308/21/104	5.6	20.0	2
							315/21/116	5.4	10.0	1

Table 1. (continued)

Event	Date[a]	Time (UT)	Seconds	Longitude	Latitude	Depth (km)	Mechanism Strike/Dip/Rake	M_w	Centroid Depth (km)	Source[b]
113	20040104	0501	35.90	−99.654	16.800	22.6	287/37/78	4.7	25.0	1
114	20040312	0152	3.50	−100.875	17.092	18.5	309/29/103	4.2	15.0	1
115	20040430	0351	56.30	−100.051	17.023	11.3	257/75/−83	3.8	10.0	1
116	20040614	2254	20.60	−98.139	16.200	17.4	277/11/70	5.9	18.0	2
							275/19/72	5.7	20.0	1
117	20041028	2030	2.00	−99.803	18.473	54.2	176/49/−89	4.8	50.0	1
118	20041115	0238	38.70	−98.659	15.980	30.0	295/21/94	5.3	12.0	2
							317/38/123	5.1	8.0	1
119	20041122	0349	25.90	−99.630	17.998	53.8	304/38/−50	4.3	50.0	1
120	20050519	0513	44.20	−98.557	16.583	44.2	88/60/−10	4.4	20.0	1
121	20050526	1555	55.70	−99.971	17.961	58.2	289/34/−76	4.6	50.0	1
122	20050814	0251	56.60	−98.385	16.023	25.1	278/16/61	5.4	12.0	2
							285/24/83	5.0	10.0	1
123	20050908	1602	1.20	−101.232	17.383	24.8	252/10/55	4.2	10.0	1
124	20050918	1125	52.30	−99.962	17.067	10.9	288/66/−47	4.0	10.0	1
125	20051202	1758	13.00	−98.489	16.378	27.6	315/48/108	4.8	20.0	1
							309/27/96	5.0	34.2	2
126	20060626	1549	18.80	−100.010	18.049	56.4	293/35/−79	4.3	50.0	1
127	20060822	1330	17.60	−99.584	17.639	1.0	261/24/−84	3.5	10.0	1
128	20070331	0618	55.80	−99.855	16.996	42.2	314/86/119	4.4	30.0	1
129	20070413	0542	21.50	−100.351	17.219	37.7	278/75/85	5.9	37.5	4
							284/73/91	5.9	38.9	2
							267/61/85	5.7	20.0	1
130	20070413	0843	45.80	−100.326	17.211	36.5	289/83/77	5.3	36.5	4
							297/90/119	5.3	66.8	2
							117/84/−101	5.3	35.0	1
131	20070428	1356	35.00	−99.836	16.999	39.9	307/75/118	4.8	30.0	1
132	20080428	0006	30.00	−101.080	17.827	61.0	317/48/−85	5.8	55.5	2
							138/40/−88	5.4	50.0	1

[a]Date is given as year, month, day.
[b]Sources are 1, focal mechanism, M_w, and centroid/constraint depth from this study; 2, focal mechanism, M_w, and centroid depth from the Global CMT catalog; 3, focal mechanism, M_w, and depth from *Pacheco and Singh* [1998]; and 4, focal mechanism, M_w, and depth from *Singh et al.* [2007].

AA′ and BB′, there are very few events of the latter type. An examination of Figure 3b, however, confirms the existence of downdip extensional earthquakes. The two types of events occur in close proximity of each other. Within the uncertainty of the locations, we do not know if the two types cluster in different depth ranges and, if so, which type occurs at shallower depth. This seismicity occurs over a small horizontal distance (∼25 km) and ceases around 105 km from the trench (∼45 km from the coast). *Suárez et al.* [1990] report a void between coastal seismicity (depth range of 10–25 km) and a second zone of inland seismicity (depth range of 32–42 km). Relocating events recorded by the same local network and during a longer time period, *Dominguez et al.* [2006] report a similar void in the seismicity. We do not find a clear evidence of the absence of seismicity, probably because Suárez et al.'s study was based on a local seismic network and had better resolution in location than the present work. If we consider ∼5 km error in our locations, then a gap of 7 km is likely to be blurred out. A speculative explanation for the void could be a deactivation of seismicity in the depth range of 25–32 km during 1986–1988, the period covered in the study of Suárez et al., and from 1987 and 1995, the period covered by the study of Dominguez et al. In view of the location error, however, this explanation, although possible, cannot be accepted.

[18] Farther inland, in the area of this study (rectangular boxes in Figure 5a, see also Figure 3b), the subducted slab is devoid of seismicity for ∼55 km. Previous studies show continuous seismic activity in this segment. We suggest this to be a consequence of projecting hypocenters of a wide area on a vertical section. Figures 3b and 5 indicate that the seismicity may not be continuous if a smaller width of 50 km is considered. The oceanic plate subducts under North America with a steep angle below Jalisco-Michoacan and an angle that decreases gradually toward the southeast [*Pardo and Suárez*, 1995]. The apparent continuity in the seismicity is a consequence of flattening of the subducted plate from west to east.

[19] The seismicity in the slab resumes with the occurrence of normal-faulting earthquakes (with stress axes showing downdip tension) in the distance range of ∼160–240 km from the trench, at a depth of ∼45–55 km (Figures 3b and 5). The low seismicity in the horizontal segment, however, is remarkable.

[20] Focal mechanisms of some of the inslab earthquakes in Table 1 differ from those discussed above. They are shown in Figure 3d. These earthquakes exhibit a large strike-slip component or dip-slip mechanisms with a strike oblique to the trench. They may represent localized stress concentrations due to contortions in the subducted plate or reactivation of old transform faults. We find event 117 (H = 50 km; Table 1) of special interest. It occurred during the operation of MASE network. Since the event was located very close to the seismic array, its depth and location are very well constrained. This event is located farther inland than any other inslab earthquake (Figures 3b and 5). The event has normal-faulting mechanism, striking N-S, almost perpendicular to the trench. This earthquake and event 63 (projected on sections AA′ in Figure 5b, even though it is located outside the box) suggest that the seismicity in the slab extends up to 240 km from the trench (Figure 5). We

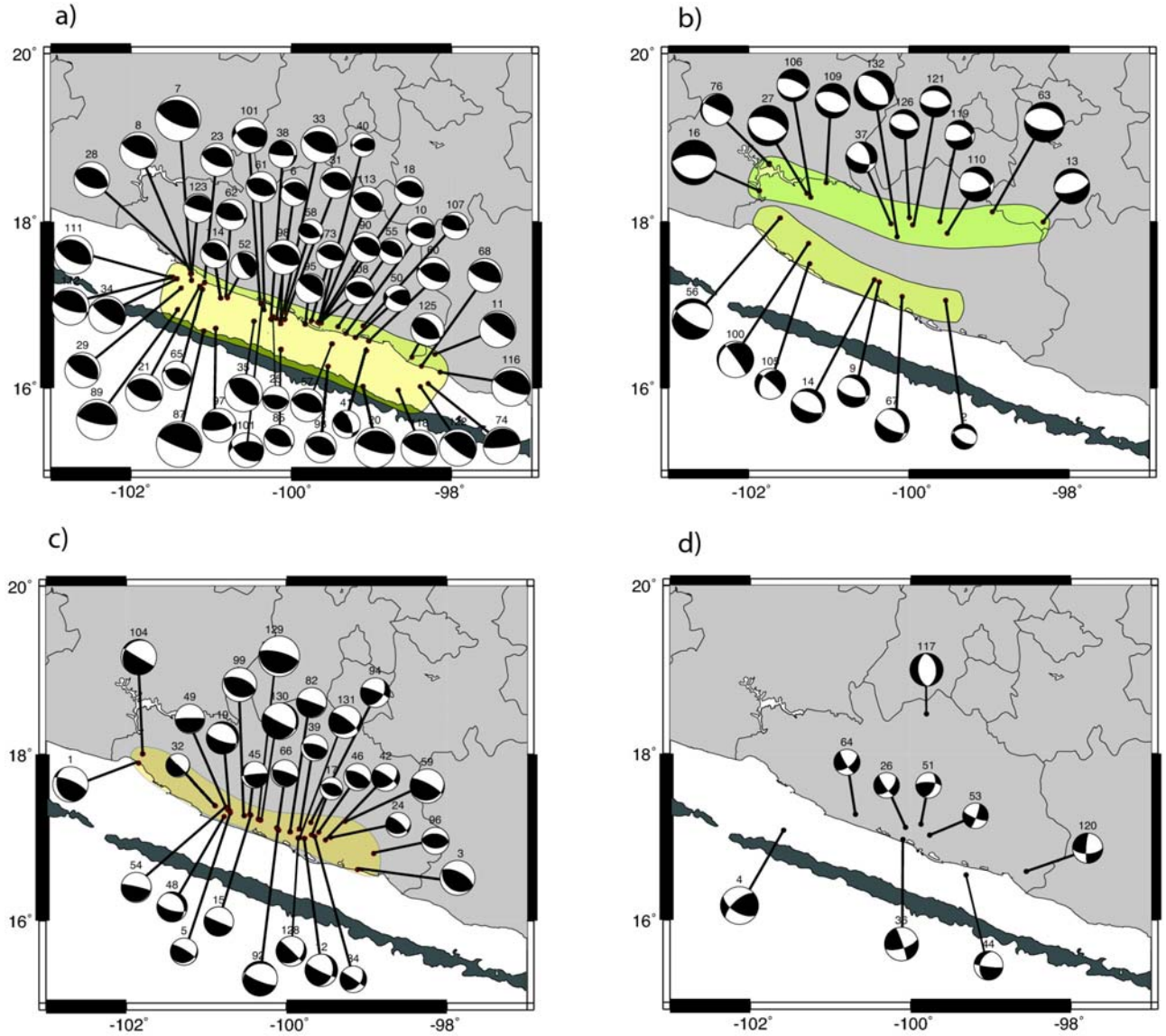

Figure 3. Epicenters and focal mechanisms of interplate and inslab earthquakes. (a) Shallow, thrust, interplate events, (b) inslab events with downdip extension, (c) inslab events with downdip compression, and (d) inslab events with unusual focal mechanism. Note that event 117 is the farthest inslab earthquake ever recorded in the Guerrero segment.

emphasize that no inslab earthquake with reliable location has been recorded beyond this distance.

3.2. Earthquakes in Overriding Plate

[21] During the time period of this study, we recorded an upper crustal earthquake (M_w 5.8; event 69, Table 1) in Coyuca de Benitez, a town close to the coast, about 20 km NW of Acapulco [*Pacheco et al.*, 2002]. Thousands of aftershocks were reported during the following 5 years, most of these too small to be well located or studied in detail. Table 1 lists the events that were located and studied in this work, and Figures 4 and 5 show their locations. Most events are shallow, with depths above 12 km. In cross section, these events depict a normal fault dipping to the south-southwest (SW) (Figure 5). Of all the crustal events reported in this study, only one (event 127 on Table 1) does not belong to the Coyuca de Benitez sequence. The event 127 is located farther inland, which is very close to the MASE array, and has a mechanism similar to those obtained for the Coyuca sequence, i.e., a normal fault striking almost parallel to the coast. *Pacheco and Singh* [1995] had previously reported a deeper event, but still within the upper crust, in a nearby region with a similar focal mechanism. These events indicate that the upper crust in the fore-arc region is under trench-normal extension, supporting previous result by *Singh and Pardo* [1993].

4. Discussion and Conclusions

4.1. Seismicity and Slab Geometry

[22] The dashed line in the sections AA′ and BB′ of Figure 5 illustrates our interpretation of the plate interface. It is based on seismicity and focal mechanisms. The plate

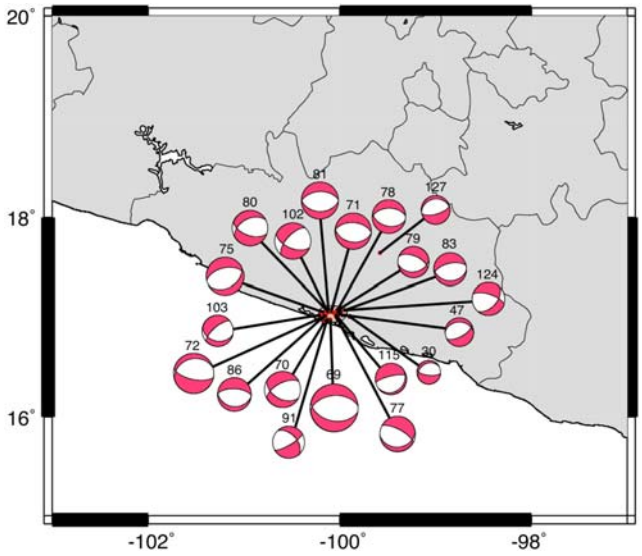

Figure 4. Epicenters and focal mechanisms of earthquakes in the upper plate.

interface follows the foci of the shallow thrust events up to ~65 km from the trench (~5 km inland). Farther inland, the interface gently unbends so that the downdip compression and extension earthquakes ($H \sim 25-45$ km) fall below the interface. We interpret the colocation of these two types of events to be a consequence of unbending for the subducted slab and draw the interface to accommodate this interpretation. In Figure 5, the interface farther inland is taken to be horizontal, with a depth of 40 km at a distance of ~110 km from the trench, and remains so at least up to 240 km. This configuration of the interface is partly based on the sparse inslab seismicity and partly on the results from the MASE data discussed below.

[23] *Pérez-Campos et al.* [2008] mapped the slab geometry below Guerrero based on RF analysis of the MASE data. This geometry is sketched on sections AA′ and BB′. As noted by Pérez-Campos et al., the slab underplates the continental crust and is almost horizontal beyond ~150 km from the trench. The northern limit of the horizontal segment is not well resolved by the RF analysis. Complementing the RF analysis with *P* wave tomography, *Pérez-Campos et al.* [2008] and *Husker and Davis* [2009] suggest that the slab remains horizontal till ~310 km from the trench, beyond which it plunges into the mantle at a steep angle, reaching a depth of 500 km at a distance of 340 km. The slab mantle in the horizontal segment is overlain by ~10 km thick anomalously low-velocity oceanic crust. This layer, in turn, is overlain by a relatively low velocity ~10 km thick layer that has been interpreted as remnant low-velocity mantle (LVM) wedge [*Pérez-Campos et al.*, 2008]. Presumably, LVM wedge also has low viscosity and low strength. The LVM wedge begins at a distance of ~125 km from the trench (Figure 5) where it is located at a depth of ~30 km. *Song et al.* [2009] studied regionally recorded converted SP phases and teleseismic underside reflections to determine the fine structure of the subducted oceanic crust below Guerrero. They report that the upper crust of the slab in the flat segment is an ultraslow velocity layer (USL), which has a shear wave velocity of 2.0–2.7 km/s and a thickness of 3–5 km. Thus, both studies indicate low-velocity subducted upper crust in the fore arc. A low-velocity upper crust in the subducted slab has also been reported in the fore arc of SW Japan [*Shelly et al.*, 2006] and Cascadia [*Bostock et al.*, 2002; *Audet et al.*, 2009].

[24] Caution is warranted in relating earthquake hypocenters and focal mechanisms reported in this study to the

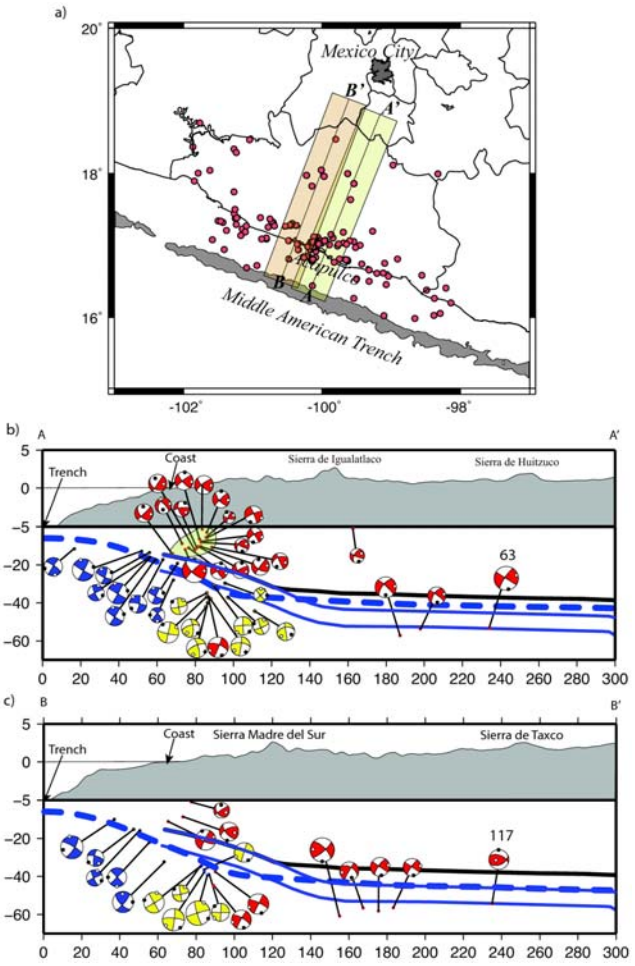

Figure 5. (a) Map of Guerrero region showing the epicenters listed in Table 1. Events which fall in the two rectangular areas are projected on vertical sections AA′ and BB′ in Figures 5b and 5c. These sections are oriented along a direction perpendicular to the trench. Each rectangle is 50 km wide. (b) Projection of hypocenters and focal mechanisms on AA′. Continuous lines sketched the slab geometry inferred from RF analysis [*Pérez-Campos et al.*, 2008]. Bottom blue line indicates top of the oceanic mantle and the layer between the two blue lines is the ocean crust. The layer contained in between the black line, and the top blue line is interpreted as mantle wedge. The dashed blue line indicates the plate interface from this work, which is in accordance with the seismicity and, with some minor deviations, the RF image. (c) Projection of hypocenters and focal mechanisms along BB′. The slab geometry is the same as in Figure 5b). In Figures 5b and 5c, focal mechanisms in blue, yellow, and red represent shallow dipping thrust, downdip compression, and downdip extensional earthquakes, respectively.

features of the slab geometry inferred for RF analysis. This is so because earthquakes have location errors of about 5 km. Furthermore, they were located using a flat layer crustal model suitable for the Guerrero region from the coast to Mexico City [*Iglesias et al.*, 2001], while the slab geometry has been mapped from RF analysis using the IASPEI Earth model as a reference. Thus, earthquake locations and RF-imaged earth structure may each be biased with respect to their true position. Modeling of regional waveforms of inslab earthquakes shows that these events occur 5 to 12 km below the USL [*Song et al.*, 2009]. This places the inslab earthquakes in the lower crust or the uppermost oceanic mantle of the slab. Thus, in the absence of relative bias, we expect the inslab earthquakes to be located in the lower oceanic crust or in the uppermost mantle of the subducted slab mapped from RF analysis. This, indeed, is supported by Figures 5b and 5c. If no relative bias exists, then we would also expect the hypocenters of shallow thrust earthquakes to fall on the plate interface. The seaward extrapolation of the RF-imaged plate interface, however, does not pass through these events (Figure 5). This may partly be due to location errors and partly due to poorly resolved RF-imaged structure near the coast owing to malfunctioning and poor quality of data from two critical coastal seismographs (X. Pérez-Campos, personal communication, 2009). The unbending of the RF-imaged slab occurs at distance of ~150 km from the trench, while inslab downdip compressional and tensional events are clustered in the distance range of 80–100 km. This large difference cannot be attributed to the error in the location of the earthquakes. Thus, if the RF-imaged slab structure is accurate in this segment, then unbending is difficult to invoke as an explanation for the change in the stress axes. Clearly, it is critical to resolve the incompatibility of the seismicity with the RF-imaged structure. This may require additional RFs near the coast, a reinterpretation of the existing ones, and an accurate three-dimensional crustal model to relocate the earthquakes.

4.2. High Pore Fluid Pressure, Upper Oceanic Crust, Slow Slip Events, Nonvolcanic Tremors, and Inslab Earthquakes

[25] Episodic SSEs and NVTs have been reported in Mexico below Guerrero [e.g., *Kostoglodov et al.*, 2003; *Iglesias et al.*, 2004; *Larson et al.*, 2007; *Payero et al.*, 2008] and Oaxaca [e.g., *Brudzinski et al.*, 2007; *Correa-Mora et al.*, 2008, 2009]. These observations bear some similarity with those documented in subduction zones of SW Japan [*Obara*, 2002; *Shelly et al.*, 2006] and Cascadia [*Dragert et al.*, 2001; *Rogers and Dragert*, 2003]. In these warm subduction zones, the SSEs and NVTs occur on the transition zone, downdip from the strongly coupled plate interface. The shear wave velocity of the upper crust of the slab in the transition zone where the SSEs occur is very low, strongly suggesting the presence of an HPFP layer. HPFP reduces effective normal stress enabling the occurrence of SSEs. Precise locations of the NVTs in SW Japan [*Shelly et al.*, 2006, 2007] and Cascadia [*La Rocca et al.*, 2009] show that they occur on the plate interface.

[26] The observations in Guerrero also reveal some important differences from those in the other two subduction zones. In SW Japan and Cascadia, SSEs and NVTs coincide spatially and temporally [e.g., *Shelly et al.*, 2006, 2007; *Rogers and Dragert*, 2003; *La Rocca et al.*, 2009]. In Guerrero, the SSEs occur in the distance range of ~90–240 km from the trench. Although limited data in Guerrero does not permit precise location of the NVTs [*Payero et al.*, 2008], they seem to occur, contemporaneous to SSEs, but only in the distance range of ~150–240 km. In SW Japan and Cascadia, inslab earthquakes occur in the lower crust or upper mantle, below the interface where SSEs take place [*Shelly et al.*, 2006; *Abers et al.*, 2009]. In Guerrero, the sparse inslab seismicity is observed in the distance range of 160–240 km but it is absent in the 90–160 km range (Figures 3b and 5), even though the SSEs occur in the entire distance range of 105–240 km. Since inslab earthquakes are linked to metamorphic dehydration reactions in the subducting oceanic crust and upper mantle [*Kirby et al.*, 1996; *Hacker et al.*, 2003], their absence in the distance range of 90–160 km suggests that these reactions begin at greater distance, in agreement with the occurrence of the NVTs and thermal models of the region [*Currie et al.*, 2002; *Manea et al.*, 2004]. The continental crust up to 250 km is characterized by high resistivity [*Jödicke et al.*, 2006], which indicates lack of, or feeble, fluid extrusion in the horizontal segment of the slab. Beyond 240 km, the relative motion on the plate interface occurs in the form of continuous creep as witnessed by the absence of the episodic SSEs. Although fluid release must be occurring beyond 240 km, the slab may be too hot ($T > 600^{\circ}$C [*Manea et al.*, 2004]) for brittle rupture.

4.3. Low Inslab Seismicity and the Plunging Slab

[27] As mentioned in section 4.1, the RF analysis, complemented with *P* wave tomography, suggests that the slab plunges into the mantle beyond ~310 km at a steep angle and reaches a depth of 500 km at a horizontal distance of ~340 km from the trench. The negative buoyancy of such a slab should give rise to extensional stress in the slab. Yet, the slab, stresswise, appears almost neutral as evidenced by only a few downdip tensional events (Figures 5b and 5c). Perhaps the slab is not continuous up to a depth of 500 km but is broken at a shallower depth, thus reducing the extensional stress in the horizontal segment of the slab. If so, then the resulting slab window may permit subslab material to flow through the gap. This could provide an explanation for recent rift-related basalts which were found along with more abundant calc-alkaline rocks in Sierra Chichinautzin, a volcanic field near Mexico City about 360 km from the trench in section AA′ of Figure 5b. An eastward propagating slab detachment below the Trans-Mexican volcanic belt (TMVB) during Miocene has been proposed by *Ferrari* [2004] to explain mafic volcanism to the north of the Pliocene-Quartenary volcanic arc. Late Miocene to present rift-related basalts are found elsewhere in the TMVB [e.g., *Verma*, 2002, 2004; *Ferrari*, 2004]. As the slab tomography along other profiles is not available, we do not know whether slab window is a viable explanation for the existence of these basalts elsewhere also.

4.4. Extensional Stress in the Overriding Plate

[28] Our study shows extensional stress in the overriding plate near the coast, as revealed by the Coyuca earthquake sequence. There is very low seismicity in the fore-arc

Table 2. Horizontal Projection of Updip and Downdip Limit of Rupture Areas (X_{TU} and X_{TD}) of Large, Shallow Thrust Earthquakes Along the Mexican Subduction Zone[a]

Event	Date[b]	Region	Latitude	Longitude	M_w	X_{TU} (km)	X_{TD} (km)	Information Used in Estimating X_{TU} and X_{TD}	Source[c]
1	30/01/1973	Colima	18.4	−103.2	7.5	50	100	Aftershocks	1
2	29/11/1978	Oaxaca	16.0	−96.7	7.8	25	82	Aftershocks	2
3	14/03/1979	Petatlan, Guerrero	17.5	−101.5	7.6	55	120	Aftershocks	3
4	25/10/1981	Playa Azul, Michoacan	17.8	−102.3	7.3	65	87	Aftershocks	4
5	07/06/1982	Ometepec, Oaxaca doublet	16.4	98.4	6.9, 7.0	40	110	Aftershocks	5
6	19/09/1985	Michoacan	18.1	−102.7	8.0	50	100	Aftershocks	6
						55	120	Waveform Inversion	7
7	21/09/1985	Guerrero-Michoacan	17.6	−101.8	7.5	40	100	Aftershocks	6
8	25/04/1989	San Marcos, Guerrero	16.6	−99.5	6.9	45	83	Aftershocks	8
9	14/09/1995	Copala, Guerrero	17.0	−99.0	7.3	40	90	Waveform Inversion	9
10	09/10/1995	Colima-Jalisco	18.8	−104.5	8.0	5	90	Aftershocks	10
						10	95	GPS data inversion	11
						0	100	Waveform Inversion	12
11	25/02/1996	Pinotepa, Oaxaca	15.6	−98.3	7.1	5	65	Aftershocks	13
12	22/01/2003	Tecoman, Colima	18.63	−104.13	7.4	40	110	Aftershocks	14
						30	100	GPS data inversion	15
						50	105	Waveform Inversion	16

[a]Distances are measured from the trench.
[b]Dates are given as day, month, year.
[c]Sources are 1, *Reyes et al.* [1979]; 2, *Singh et al.* [1980]; 3, *Valdés-González and Novelo-Casanova* [1998]; 4, *Havskov et al.* [1983]; 5, E. Nava (personal communication, 1985); 6, *UNAM Seismology Group* [1986]; 7, *Mendoza and Hartzell* [1989]; 8, *Singh et al.* [1989]; 9, *Courboulex et al.* [1997]; 10, *Pacheco et al.* [1997]; 11, *Melbourne et al.* [1997], *Hutton et al.* [2001], and *Schmitt et al.* [2007]; 12, *Mendoza and Hartzell* [1999]; 13, M. Islas (personal communication, 1997); 14, *Singh et al.* [2003]; 15, *Schmitt et al.* [2007]; and 16, *Yagi et al.* [2004].

region. The few earthquakes which have been recorded between the coast and the Mexican Volcanic Belt reveal that the upper plate is in tension. This is supported by geological studies, which report no compressional geologic features in the fore arc in the last 20 Ma [e.g., *Nieto-Samaniego et al.*, 2006; *Morán-Zenteno et al.*, 2007]. The extensional stress in the overriding plate of this convergent margin may be explained by tectonic erosion and/or seaward migration of the trench, as previously suggested by *Singh and Pardo* [1993]. Tectonic erosion characterizes the Middle American subduction zone [e.g., *Clift and Vannucchi*, 2004], especially the Acapulco trench where geologic features are truncated [e.g., *Ducea et al.*, 2004]. Tensional stresses on the upper plate close to the coast and above the transition between the brittle section and stable sliding or plastic creep along the plate interface might come about from gravitational collapse due to tectonic erosion. In this respect, the northern Chilean subduction zone presents characteristics similar to the one in Guerrero. Tectonic erosion and underplating is present in Chile [*von Huene and Ranero*, 2003; *Clift and Hartley*, 2007] and active normal faulting on the overriding plate is currently occurring [*Delouis et al.*, 1998; *González et al.*, 2003]. On the other hand, volcanism in the Mexican Volcanic Belt has migrated to the south at the rate of 9.4 km/Ma [*Ferrari et al.*, 2001]. Seaward retreat of the Middle America trench and rollback of the steeply-dipping slab provide two possible mechanisms for the migration.

4.5. Width of Seismogenic Plate Interface in Guerrero

[29] A critical issue in the estimation of tsunami and seismic hazard in the Guerrero region is the updip and downdip limits of the plate interface that can rupture during large/great shallow thrust earthquakes in the region. Several previous studies report a very narrow width of the plate interface along the Middle American subduction zone in southern Mexico [e.g., *Singh et al.*, 1985; *Singh and Mortera*, 1991; *Pacheco et al.*, 1993; *Tichelaar and Ruff*, 1993; *Suárez and Sánchez*, 1996; *Valdés-Gonzalez and Meyer*, 1996; *Valdés-González and Novelo-Casanova*, 1998]. However, the rupture limits are still poorly known. As the seismographs and GPS stations are located on land, the updip limit is not well constrained. The shallow interplate seismicity in Guerrero ends about 65 km from the trench at 25 km depth (Figures 5b and 5c). This would be the downdip limit of the rupture if the relative plate motion further downdip occurs as postseismic slip or during episodic SSEs. The downdip limit of small, shallow thrust events, however, may not coincide with the updip limit of the interface where relative motion occurs during SSEs. Precise knowledge of the spatial distribution of slip during SSEs is needed to resolve this issue. This, however, is not the case in Guerrero due to sparse GPS data. In particular, the updip extent of the slip during SSEs (hence, the downdip limit of rupture during large/great earthquakes) is not well constrained [*Iglesias et al.*, 2004; *Yoshioka et al.*, 2004; *Correa-Mora et al.*, 2009]. *Peacock and Hyndman* [1999] suggest that the downdip limit of the rupture extends up to the point where the ocean crust intersects with the mantle wedge. As mentioned in section 4.1, *Pérez-Campos et al.* [2008] interpret the relatively low-velocity, 10 km thick layer above the ocean crust as mantle wedge (Figure 5). This suggests that the downdip limit in Guerrero would be located ∼125 km from the trench at a depth of ∼30 km. This estimate differs considerably from the one based on shallow thrust seismicity.

[30] Tide records of the Guerrero doublet of 11 May (M_w 7.1) and 19 May 1962 (M_w 7.0) at Acapulco have been used to estimate the rupture dimension of these events [*Ortiz et al.*, 2000]. The tide gauge was located in or near the epicentral region of the earthquakes. The events caused a coastal uplift of 15 ± 3 cm and 11 ± 3 cm, respectively, indicating that part of the slip areas were located onshore.

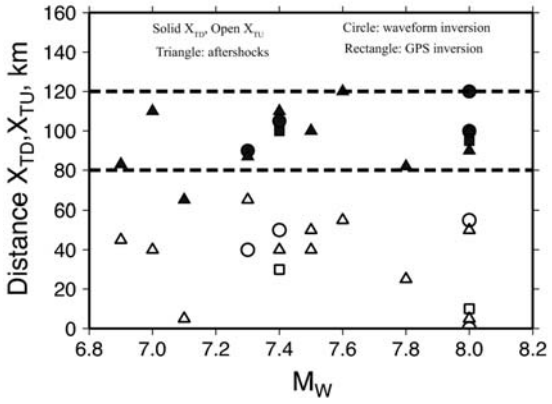

Figure 6. Horizontal projection of updip and downdip limits of rupture areas (X_{TU} and X_{TD}) of large, shallow thrust earthquakes along the Mexican subduction zone. Data are from Table 2. Distances are measured from the trench. Dashed lines show the range of observed X_{TD} (between 80 and 120 km), with the exception of the earthquake of 25 February 1997 (M_w 7.1) (Table 2).

Let X_{TU} and X_{TD} be the horizontal distance from the trench to updip and downdip extent of a rupture area, respectively. The modeling of the tide records of the two earthquakes yields X_{TU} = 60 km and X_{TD} = 90 km [*Ortiz et al.*, 2000].

[31] Rupture areas of large/great earthquakes along other segments of the Mexican subduction zone, estimated from aftershocks, and spatial distribution of coseismic slip obtained from inversion of GPS data and/or waveforms, may also provide information on what might be expected in Guerrero. Figure 1 outlines rupture areas of recent Mexican earthquakes and Table 2 lists their X_{TU} and X_{TD} values. Figure 6 shows a plot of X_{TU} and X_{TD} as a function of M_w. The estimates of rupture areas are subject to uncertainty. In particular, aftershock area grows with time [see, e.g., *Tajima and Kanamori*, 1985]. For many of the earthquakes listed in Table 2, the aftershock area is the only information available. However, for three earthquakes, the estimates are available from at least two data sets. In these cases, X_{TU} and X_{TD} from different data sets are roughly the same, especially X_{TD}. Furthermore, *Correa-Mora et al.* [2008] report that SSEs in Oaxaca are occurring immediately downdip from the aftershock area of the 1978 earthquake (M_w 7.8), entirely relieving the accumulated strain energy. The aftershock area of the 1978 earthquake itself is presently completely locked. This gives us some confidence that the estimated X_{TD} values in Table 2 (and to a lesser degree X_{TU}) are reasonably reliable. From Figure 6, we find that $80 \leq X_{TD} \leq 120$ km, with one exception. Thus, different estimates of the upper limit of X_{TD} during large/great earthquakes in Guerrero are possible: X_{TD} = 65 km from shallow seismicity; X_{TD} = 90 km from the 1962 earthquakes; X_{TD} = 120 km from rupture areas of adjacent segments; and X_{TD} = 125 km from the possible location of the mantle wedge. Perhaps $X_{TD} = 105 \pm 15$ km adequately reflects our current knowledge of downdip limit of the rupture in Guerrero. An updip limit of X_{TU} of 5 km in Guerrero would provide a conservative estimation of tsunami hazard in the region.

4.6. Seismic Hazard in Guerrero From Sources Other Than Interplate Earthquakes

[32] Apart from interplate, shallow thrust earthquakes, Guerrero also faces seismic hazard from the two types of inslab events below the coast: the downdip compression type and the downdip extension type. The downdip extensional events may reach M_w of about 7.5. Recent examples of this type of earthquake along the Mexican subduction zone are: 30 January 1997 Michoacan earthquake (M_w 7.1) and 30 September 1999 Oaxaca earthquake (M_w 7.4). The compressional type of earthquake could reach a magnitude M_w of 6.5. Examples of such events are: 3 February 1998 earthquake of Oaxaca (M_w 6.3), 9 August 2000 earthquake of Michoacan (M_w 6.5) and 13 April 2007 earthquake of Atoyac, Guerrero (M_w 5.9; event 129, Table 1). We note that inslab earthquakes in Mexico are more energetic at higher frequency than interplate events and, hence, follow a separate ground motion attenuation relation [*García et al.*, 2004, 2005]. Finally, the normal-faulting, shallow crustal earthquakes, such as that of Coyuca, need to be considered in seismic hazard estimation. Unfortunately, the recurrence period of these and the inslab earthquakes is not known.

[33] **Acknowledgments.** This work would not have been possible without the dedication of many persons involved in the operation of the three networks whose data were used in this study. In particular, we thank Jorge Estrada, José Luis Cruz, and Jesús Pérez Santana who maintain the broadband seismic network of the SSN; Leonardo Alcántara, David Almora, Miguel Torres, Ricardo Vásquez, Juan Manuel Velazco, and Mauricio Ayala for the Guerrero strong motion network; and Arturo Iglesias and Xyoli Pérez for maintaining the MASE array. Comments by two anonymous referees helped us in significantly improving the manuscript. Discussions with Xyoli Pérez, and Dave Scholl were fruitful to us. We especially thank Joan Gomberg for her thoughtful remarks. Some of the figures were prepared with the GMT package of *Wessel and Smith* [1995]. This research was partly supported by CONACYT projects 36671 and 82595.

References

Abers, G. A., L. S. MacKenzie, S. Rondenay, Z. Zhang, and A. G. Wech (2009), Imaging the source region of Cascadia tremor and intermediate-depth earthquakes, *Geology*, *37*, 1119–1122, doi:10.1130/G30143A.1.

Anderson, J. G., J. N. Brune, J. Prince, R. Quaas, S. K. Singh, D. Almora, P. Bodin, M. Oñate, R. Vásquez, and J. M. Velasco (1994), The Guerrero accelerograph network, *Geofis. Int.*, *33*, 341–371.

Audet, P., M. G. Bostock, N. I. Christensen, and S. M. Peacock (2009), Seismic evidence for overpressured subducted oceanic crust and megathrust fault sealing, *Nature*, *457*, 76–78, doi:10.1038/nature07650.

Bostock, M. G., R. D. Hyndman, S. Rondenay, and S. M. Peacock (2002), An inverted continental Moho and serpentinization of the forearc mantle, *Nature*, *417*, 536–538, doi:10.1038/417536a.

Brudzinski, M., E. Cabral-Cano, F. Correa-Mora, C. DeMets, and B. Márquez-Azúa (2007), Slow slip transients along the Oaxaca subduction segment from 1993 to 2007, *Geophys. J. Int.*, *171*, 523–538.

Clayton, R., P. M. Davis, and X. Pérez-Campos (2007), Seismic structure of the subducted Cocos plate, *Eos Trans. AGU*, *88*(23), Jt. Assem. Suppl., Abstract T32A-01.

Clift, P. D., and A. J. Hartley (2007), Slow rates of subduction erosion and coastal underplating along the Andean margin of Chile and Peru, *Geology*, *35*, 503–506, doi:10.1130/G23584A.1.

Clift, P. D., and P. Vannucchi (2004), Controls on tectonic accretion versus erosion in subduction zones: Implications for the origin and recycling of the continental crust, *Rev. Geophys.*, *42*, RG2001, doi:10.1029/2003RG000127.

Correa-Mora, F., C. DeMets, E. Cabral-Cano, B. Marquez-Azua, and O. Diaz-Molina (2008), Interplate coupling and transient slip along the subduction interface beneath Oaxaca, Mexico, *Geophys. J. Int.*, *175*, 269–290.

Correa-Mora, F., C. DeMets, E. Cabral-Cano, O. Diaz-Molina, and B. Marquez-Azua (2009), Transient deformation in southern Mexico in 2006 and 2007: Evidence for distinct deep-slip patches beneath Guerrero

and Oaxaca, *Geochem. Geophys. Geosyst.*, *10*, Q02S12, doi:10.1029/2008GC002211.

Courboulex, F., M. A. Santoyo, J. F. Pacheco, and S. K. Singh (1997), The 14 September 1995 (M = 7.3) Copala, Mexico, earthquake: A source study using teleseismic, regional, and local data, *Bull. Seismol. Soc. Am.*, *87*, 999–1010.

Currie, C. A., R. D. Hyndman, K. Wang, and V. Kostoglodov (2002), Thermal models of the Mexico subduction zone: Implications for the megathrust seismogenic zone, *J. Geophys. Res.*, *107*(B12), 2370, doi:10.1029/2001JB000886.

Delouis, B., H. Philip, L. Dorbath, and A. Cisternas (1998), Recent crustal deformation in the Antofagasta region (northern Chile) and the subduction process, *Geophys. J. Int.*, *132*, 302–338, doi:10.1046/j.1365-246x.1998.00439.

Dominguez, J., G. Suárez, D. Comte, and L. Quintanar (2006), Seismic velocity structure of the Guerrero gap, Mexico, *Geofis. Int.*, *45*, 129–139.

Dragert, H., K. Wang, and T. S. James (2001), A silent slip event on the deeper Cascadia subduction interface, *Science*, *292*, 1522–1528.

Ducea, M., V. A. Valencia, S. Shoemaker, P. W. Reiners, P. G. DeCelles, M. F. Campa, and D. Moran-Zenteno (2004), Rate of sediment recycling beneath the Acapulco trench: Constraints from (U-Th)/He thermochronology, *J. Geophys. Res.*, *109*, B09404, doi:10.1029/2004JB003112.

Dziewonski, A. M., and J. H. Woodhouse (1983), An experiment in the systematic study of global seismicity: Centroid-moment tensor solutions for 201 moderate and large earthquakes of 1981, *J. Geophys. Res.*, *88*, 3247–3271.

Ferrari, L. (2004), Slab detachment control on mafic volcanic pulse and mantle heterogeneity in central Mexico, *Geology*, *32*, 77–80.

Ferrari, L., C. M. Petrone, and L. Francalanci (2001), Generation of oceanic-island basalt-type volcanism in the western Trans-Mexican volcanic belt by slab rollback, asthenosphere infiltration, and variable flux melting, *Geology*, *29*, 507–510.

García, D., S. K. Singh, M. Herráiz, J. F. Pacheco, and M. Ordaz (2004), Inslab earthquakes of central Mexico: Q, source spectra and stress drop, *Bull. Seismol. Soc. Am.*, *94*, 789–802.

García, D., S. K. Singh, M. Herráiz, M. Ordaz, and J. F. Pacheco (2005), Inslab earthquakes of central Mexico: Peak ground-motion parameters and response spectra, *Bull. Seismol. Soc. Am.*, *95*, 2272–2282.

González, G., J. Cembrano, D. Carrizo, A. Macci, and H. Schneider (2003), The link between forearc tectonics and Pliocene-Quaternary deformation of the coastal Cordillera, northern Chile, *J. South Am. Earth Sci.*, *16*, 321–342, doi:10.1016/S0895-9811(03)00100-7.

González-Ruiz, J. R. (1986), Earthquake source mechanics and tectonophysics of the middle America subduction zone in Mexico, Ph.D. thesis, Univ. of Calif., Santa Cruz.

Hacker, B. R., S. M. Peacock, G. A. Abers, and S. D. Holloway (2003), Subduction factory: 2. Are intermediate-depth earthquakes in subducting slabs linked to metamorphic dehydration reactions?, *J. Geophys. Res.*, *108*(B1), 2030, doi:10.1029/2001JB001129.

Havskov, J., and L. Ottemöller (1999), Electronic seismologist: SeisAn earthquake analysis software, *Seismol. Res. Lett.*, *70*, 532–534.

Havskov, J., S. K. Singh, E. Nava, T. Domínguez, and M. Rodríguez (1983), Playa Azul, Michoacan, Mexico earthquake of 25 October 1981, (M_s = 7.3), *Bull. Seismol. Soc. Am.*, *73*, 449–457.

Husker, A., and P. M. Davis (2009), Tomography and thermal state of the Cocos plate subduction beneath Mexico City, *J. Geophys. Res.*, *114*, B04306, doi:10.1029/2008JB006039.

Hutton, W., C. DeMets, O. Sanchez, G. Suarez, and J. Stock (2001), Slip kinematics and dynamics during and after the 1995 October 9 M_w = 8.0 Colima-Jalisco earthquake, Mexico, from GPS geodetic constraints, *Geophys. J. Int.*, *146*, 637–658.

Iglesias, A., V. M. Cruz-Atienza, N. M. Shapiro, S. K. Singh, and J. F. Pacheco (2001), Crustal structure of south-central Mexico estimated from the inversion of surface-wave dispersion curves using genetic and simulated annealing algorithms, *Geofis. Int.*, *40*, 181–190.

Iglesias, A., S. K. Singh, A. R. Lowry, M. Santoyo, V. Kostoglogov, K. M. Larson, and S. I. Franco-Sanchéz (2004), The silent earthquake of 2002 in the Guerrero seismic gap, Mexico (Mw = 7.6): Inversion of slip on the plate interface and some implications, *Geofis. Int.*, *43*, 309–317.

Jödicke, H., A. Jording, L. Ferrari, J. Arzate, K. Mezger, and L. Rüpke (2006), Fluid release from the subducted Cocos plate and partial melting of the crust deduced from magnetotelluric studies in southern Mexico: Implications for the generation of volcanism and subduction dynamics, *J. Geophys. Res.*, *111*, B08102, doi:10.1029/2005JB003739.

Kelleher, J., L. Sykes, and J. Oliver (1973), Possible criteria for predicting earthquake locations and their application to major plate boundaries in the Pacific and the Caribbean, *J. Geophys. Res.*, *78*, 2547–2585.

Kirby, S. H., E. R. Engdahl, and R. Denlinger (1996), Intermediate intraslab earthquakes and arc volcanism as physical expressions of crustal and upper mantle metamorphism in subducting plates, in *Subduction: Top to Bottom*, *Geophys. Monogr. Ser.*, vol. 96, edited by G. Bebout, D. Scholl, and S. Kirby, pp. 195–214, AGU, Washington, D. C.

Kodaira, S., T. Iidaka, A. Kato, J. O. Park, T. Iwasaki, and Y. Kaneda (2004), High pore fluid pressure may cause silent slip in the Nakai Trough, *Science*, *304*, 1295–1298.

Kostoglodov, V., S. K. Singh, J. A. Santiago, S. I. Franco, K. M. Larson, A. R. Lowry, and R. Bilham (2003), A large silent earthquake in the Guerrero seismic gap, Mexico, *Geophys. Res. Lett.*, *30*(15), 1807, doi:10.1029/2003GL017219.

La Rocca, M., K. C. Creager, D. Galluzzo, S. Malone, J. E. Vidale, J. R. Sweet, and A. G. Wech (2009), Cascadia tremor located near plate interface constrained by S minus P wave times, *Science*, *323*, 620–623, doi:10.1126/science.1167112.

Larson, K., V. Kostoglodov, S. Miyazaki, and J. Santiago (2007), The 2006 aseismic slow slip event in Guerrero, Mexico: New results from GPS, *Geophys. Res. Lett.*, *34*, L13309, doi:10.1029/2007GL029912.

Lienert, B. R., and J. Havskov (1995), A computer program for locating earthquakes both locally and globally, *Seismol. Res. Lett.*, *66*, 26–36.

Manea, V. C., M. Manea, V. Kostoglodov, C. A. Currie, and G. Sewell (2004), Thermal structure, coupling and metamorphism in the Mexican subduction zone beneath Guerrero, *Geophys. J. Int.*, *158*, 775–784, doi:10.1111/j.1365-246X.2004.02325x.

Melbourne, T., I. Carmichael, C. De Mets, K. Hudnut, O. Sanchez, J. Stock, G. Suarez, and F. Webb (1997), The geodetic signature of the M 8.0 October 9, 1995, Colima-Jalisco, Mexico, *Geophys. Res. Lett.*, *24*, 715–718.

Mendoza, C., and S. Hartzell (1989), Slip distribution of the 19 September 1985 Michoacan, Mexico, earthquake: Near-source and teleseismic constraints, *Bull. Seismol. Soc. Am.*, *79*, 655–669.

Mendoza, C., and S. Hartzell (1999), Fault-slip distribution of the 1995 Colima-Jalisco, Mexico, earthquake, *Bull. Seismol. Soc. Am.*, *89*, 1338–1344.

Molnar, P., and L. R. Sykes (1969), Tectonics of the Caribbean and Middle American region from focal mechanisms and seismicity, *Geol. Soc. Am. Bull.*, *80*, 1639–1684.

Morán-Zenteno, D. J., M. Cerca, and J. D. Keppie (2007), The Cenozoic tectonic and magmatic evolution of southwestern Mexico: Advances and problem of interpretation, in *Geology of Mexico, Celebrating the Centenary of the Geological Society of Mexico*, edited by S. A. Alaniz-Alvarez and A. F. Nieto-Samaniego, *Spec. Pap. Geol. Soc. Am.*, *422*, 71–91.

Nieto-Samaniego, A. F., A. S. Alaniz-Alvarez, G. Silva-Romo, M. H. Eguiza-Castro, and C. Mendoza-Rosales (2006), Latest Cretaceous to Miocene deformation events in the eastern Sierra Madre del Sur, Mexico, inferred from the geometry and age of major structures, *Geol. Soc. Am. Bull.*, *118*, 238–252.

Obara, K. (2002), Nonvolcanic deep tremor associated with subduction in southwest Japan, *Science*, *296*, 1679–1681.

Ortiz, M., S. K. Singh, V. Kostoglodov, and J. F. Pacheco (2000), Source areas of the Acapulco-SanMarcos, México earthquakes of 1962 (M 7.1; 7.0) and 1957 (M 7.7) as constrained by tsunami and uplift records, *Geofis. Int.*, *39*, 337–348.

Pacheco, J. F., and S. K. Singh (1995), El Temblor de Iguala del 2 de Septiembre de 1995 (M = 3.8): Implicaciones sobre el estado de esfuerzos en la corteza superior al sur de México, *GEOS*, *15*, 54.

Pacheco, J. F., and S. K. Singh (1998), Source parameters of two moderate Mexican earthquakes estimated from a single-station, near-source recording, and from MT inversion of regional data: A comparison of the results, *Geofis. Int.*, *37*, 95–102.

Pacheco, J. F., L. Sykes, and C. Scholz (1993), Nature of seismic coupling along simple plate boundaries of the subduction type, *J. Geophys. Res.*, *98*, 14,133–14,159.

Pacheco, J. F., et al. (1997), The October 9, 1995 Colima-Jalisco, Mexico, earthquake (M_w 8): An aftershock study and a comparison of this earthquake with those of 1932, *Geophys. Res. Lett.*, *24*, 2223–2226.

Pacheco, J. F., C. A. Mortera-Gutiérrez, H. Delgado, S. K. Singh, R. W. Valenzuela, N. M. Shapiro, M. A. Santoyo, A. Hurtado, R. Barrón, and E. Gutiérrez-Moguel (1999), Tectonic significance of an earthquake sequence in the Zacoalco half-graben, Jalisco, Mexico, *J. South Am. Earth Sci.*, *12*, 557–565.

Pacheco, J. F., A. Iglesias, S. K. Singh, C. Gutiérrez, G. Espitía, and L. Alcántara (2002), The 8 October 2001 Coyuca, Guerrero, México Earthquake (M_w 5.9): A normal fault in an expected compressional environment, *Seismol. Res. Lett.*, *73*, 263.

Pardo, M., and G. Suárez (1995), Shape of the subducted Rivera and Cocos plates in southern Mexico: Seismic and tectonic implications, *J. Geophys. Res.*, *100*, 12,357–12,373.

Payero, J., V. Kostoglodov, N. Shapiro, T. Mikumo, A. Iglesias, X. Pérez-Campos, and R. Clayton (2008), Non-volcanic tremor observed

in the Mexican subduction zone, *Geophys. Res. Lett.*, *35*, L07305, doi:10.1029/2007GL032877.

Peacock, S. M., and R. D. Hyndman (1999), Hydrous minerals in the mantle wedge and the maximum depth of subduction thrust earthquakes, *Geophys. Res. Lett.*, *26*, 2517–2520.

Pérez-Campos, X., Y. H. Kim, A. Husker, P. M. Davis, R. W. Clayton, A. Iglesias, J. F. Pacheco, S. K. Singh, V. C. Manea, and M. Gurnis (2008), Horizontal subduction and truncation of the Cocos plate beneath central Mexico, *Geophys. Res. Lett.*, *35*, L18303, doi:10.1029/2008GL035127.

Randall, G. E., C. J. Ammon, and T. J. Owens (1995), Moment tensor estimation using regional seismograms form a Tibetan Plateau portable network deployment, *Geophys. Res. Lett.*, *22*, 1665–1668.

Reyes, A., J. N. Brune, and C. Lomnitz (1979), Source mechanism and aftershock study of the Colima, Mexico earthquake of January 30, 1973, *Bull. Seismol. Soc. Am.*, *69*, 1819–1840.

Rogers, G., and H. Dragert (2003), Episodic tremor and slip on the Cascadia subduction zone: The chatter of silent slip, *Science*, *300*, 1942–1943.

Santoyo, M. A., S. K. Singh, and T. Mikumo (2005), Source process and stress change associated with the 11 January, 1997 (M_w = 7.1) Michoacán, México, inslab earthquake, *Geofis. Int.*, *44*, 317–330.

Schmitt, S. V., C. DeMets, J. Stock, O. Sanchez, and B. Marquez-Azua (2007), A geodetic study of the 2003 January 22 Tecoman, Colima, Mexico earthquake, *Geophys. J. Int.*, *169*, 389–406, doi:10.1111/j.1365-246X.2006.03322.x.

Shelly, D. M., G. C. Beroza, S. Ide, and S. Nakamula (2006), Low-frequency earthquakes in Shikoku, Japan, and their relationship to episodic tremor and slip, *Nature*, *442*, 188–191, doi:10.1038/nature04931.

Shelly, D. M., G. C. Beroza, and S. Ide (2007), Non-volcanic tremor and low-frequency earthquake swarms, *Nature*, *446*, 305–307, doi:10.1038/nature05666.

Singh, S. K., and F. Mortera (1991), Source time functions of large Mexican subduction earthquakes, morphology of the Benioff zone, age of the plate and their tectonic implications, *J. Geophys. Res.*, *96*, 21,487–21,502.

Singh, S. K., and M. Pardo (1993), Geometry of the Benioff Zone and state of stress in the overriding plate in central Mexico, *Geophys. Res. Lett.*, *20*, 1483–1486.

Singh, S. K., J. Havskov, K. McNally, L. Ponce, T. Hearn, and M. Vassiliou (1980), The Oaxaca, Mexico earthquake of 19 November, 1978: A preliminary report on aftershocks, *Science*, *207*, 1211–1213.

Singh, S. K., L. Astiz, and J. Havskov (1981), Seismic gaps and recurrence periods of large earthquakes along the Mexican subduction zone: A reexamination, *Bull. Seismol. Soc. Am.*, *71*, 827–843.

Singh, S. K., G. Suarez, and T. Dominguez (1985), The Oaxaca, Mexico earthquake of 1931: Lithospheric normal faulting in the subducted Cocos plate, *Nature*, *137*, 56–58.

Singh, S. K., M. Ordaz, R. Quaas, and E. Mena (1989), Estudio preliminar de la fuente del temblor del 25 de Abril de 1989 (M_s 6.9) a partir de los datos de movimientos fuertes, in *Memoires VIII Congreso Nacional de Ingenieria Sismica y VII Congreso Nacional de Ingenieria Estructural*, vol. I, pp. A199–A211, Natl. Seismic Eng., Mexico City.

Singh, S. K., M. Ordaz, J. F. Pacheco, and F. Courboulex (2000a), A simple source inversion scheme for displacement seismograms recorded at short distances, *J. Seismol.*, *4*, 267–284.

Singh, S. K., et al. (2000b), The Oaxaca earthquake of September 30, 1999 (M_w = 7.5): A normal faulting event in the subducted Cocos plate, *Seismol. Res. Lett.*, *71*, 67–78.

Singh, S. K., et al. (2003), A preliminary report on the Tecomán, México earthquake of 22 January 2003 (M_w 7.4) and its effects, *Seismol. Res. Lett.*, *74*, 280–290.

Singh, S. K., M. Ordaz, J. F. Pacheco, L. Alcántara, A. Iglesias, S. Alcocer, D. García, X. Pérez-Campos, C. Valdes, and D. Almora (2007), A report on the Atoyac, Mexico, earthquake of 13 April 2007 (*M* 5.9), *Seismol. Res. Lett.*, *78*, 635–648.

Song, T. R. A., D. V. Helmberger, M. R. Brudzinski, R. W. Clayton, P. Davis, X. Pérez-Campos, and S. K. Singh (2009), Subducting slab ultra-slow velocity layer coincident with silent earthquakes in southern Mexico, *Science*, *324*, 502–506.

Suárez, G., and O. Sánchez (1996), Shallow depth of seismogenic coupling in southern Mexico: Implications for the maximum size of earthquakes in the subduction zone, *Phys. Earth Planet. Inter.*, *93*, 53–61.

Suárez, G., T. Monfret, G. Wittlinger, and C. David (1990), Geometry of subduction and depth of the seismogenic zone in the Guerrero gap, Mexico, *Nature*, *345*, 336–338.

Tajima, F., and H. Kanamori (1985), Global survey of aftershock area expansion patterns, *Phys. Earth Planet. Inter.*, *40*, 77–134.

Tichelaar, B., and L. Ruff (1993), Depth of seismic coupling along subductions zones, *J. Geophys. Res.*, *98*, 2017–2037.

UNAM Seismology Group (1986), The September 1985 Michoacan earthquakes: Aftershock distribution and history of rupture, *Geophys. Res. Lett.*, *13*, 573–576.

Valdés-Gonzalez, C., and R. P. Meyer (1996), Seismic structure between the Pacific coast and Mexico City from the Petatlán earthquake (M_s = 7.6) aftershocks, *Geofis. Int.*, *35*, 377–401.

Valdés-González, C., and D. A. Novelo-Casanova (1998), The western Guerrero, Mexico, seismogenic zone from the microseismicity associated to the 1979 Petatlan and 1985 Zihuatanejo earthquakes, *Tectonophysics*, *287*, 271–277, doi:10.1016/S0040-1951(98)80073-5.

Verma, S. P. (2002), Absence of Cocos plate subduction-related basic volcanism in southern Mexico: A unique case on Earth?, *Geology*, *30*, 1095–1098.

Verma, S. P. (2004), Solely extension-related origin of the eastern to west-central Mexican volcanic belt (Mexico) from partial melting inversion model, *Curr. Sci.*, *86*, 713–719.

von Huene, R., and C. Ranero (2003), Subduction erosion and basal friction along the sediment-starved convergent margin on Antofagasta, Chile, *J. Geophys. Res.*, *108*(B2), 2079, doi:10.1029/2001JB001569.

Wessel, P., and W. H. F. Smith (1995), New version of the generic mapping tools released, *Eos Trans. AGU*, *76*, 329.

Yagi, Y., T. Mikumo, J. Pacheco, and G. Reyes (2004), Source rupture process of the Tecomán, Colima, México earthquake of 22 January 2003, determined by joint inversion of teleseismic body-wave and near-source data, *Bull. Seismol. Soc. Am.*, *94*, 1795–1807.

Yoshioka, Y., T. Mikumo, V. Kostoglodov, K. M. Larson, A. R. Lowry, and S. K. Singh (2004), Interplate coupling and a recent aseismic slow slip event in the Guerrero seismic gap of the Mexican subduction zone, as deduced from GPS data inversion using a Bayesian information criterion, *Phys. Earth Planet. Inter.*, *146*, 513–530, doi:10.1016/j.pepi.2004.05.006.

J. F. Pacheco, Observatorio Vulcanológico y Sismológico de Costa Rica, Universidad Nacional Autónoma, Heredia, Costa Rica. (jpacheco@una.ac.cr)

S. K. Singh, Instituto de Geofísica, Universidad Nacional Autónoma de México, Ciudad Universitaria, C.P. 04510, Del. Coyoacán, México D. F., México.